Electronic Supplementary Material (ESI) for Journal of Materials Chemistry C.

SUPPORTING INFORMATION

Reversible redox reactions in metal-supported porphyrin: the role of spin and oxidation state

Iulia Cojocariu,*[a] Silvia Carlotto,*[b,c] Giovanni Zamborlini, #[a] Matteo Jugovac,$[a] Luca Schio,[d] Luca Floreano,[d] Maurizio Casarin,[b] Vitaliy Feyer,*[a,e] and Claus M. Schneider[a,e]

[a] I. Cojocariu, Dr. G. Zamborlini, Dr. M. Jugovac, Dr. V. Feyer, Prof. C. M. Schneider
Peter Grünberg Institute (PGI-6), Forschungszentrum Jülich GmbH, Leo-Brandt-Straße, 52428 Jülich, Germany
E-mail: i.cojocariu@fz-juelich.de; v.feyer@fz-juelich.de

[b] Dr. S. Carlotto, Prof. M. Casarin
Dipartimento di Scienze Chimiche, Università degli Studi di Padova, via F. Marzolo 1, 35131 Padova, Italy
E-mail: silvia.carlotto@unipd.it

[c] Dr. S. Carlotto
Institute of Condensed Matter Chemistry and Technologies for Energy (ICMATE), National Research Council (CNR), c/o Department of Chemistry, University of Padova, via F. Marzolo 1, 35131 Padova, Italy

[d] Dr. L. Schio, Dr. L. Floreano
CNR-IOM, Lab. TASC, s.s. 14 km 163,5, 34149 Trieste, Italy

[e] Dr. V. Feyer, Prof. C. M. Schneider
Fakultät f Physik and Center for Nanointegration Duisburg-Essen (CENIDE), Universität Duisburg-Essen, D-47048 Duisburg, Germany

Present address: Technische Universität Dortmund, Experimentelle Physik VI, 44227 Dortmund, Germany

$ Present address: Istituto di Struttura della Materia-CNR (ISM-CNR), 34149 Trieste, Italy

Experimental Procedures and Computational details

The valence band photoemission spectra were measured at the NanoESCA beamline of Elettra, the Italian synchrotron radiation facility in Trieste, using an electrostatic photoemission electron microscope (PEEM) set-up described in detail in Ref. [1]. The data were collected with a photon energy of 30 eV and a total energy resolution of 100 meV, using *p*-linearly polarized light.
The XPS and NEXAFS measurements were carried out at the ALOISA beamline situated at the Elettra synchrotron radiation facility in Trieste[2].
The NEXAFS spectra across the N K-edge and Co L-edge were taken in partial electron yield operation mode using a channeltron multiplier[2]. The photon flux normalization and the energy calibration of the NEXAFS data have been performed following the procedure described in ref. [3]. The orientation of the surface with respect to the linear polarization (s and p) of the synchrotron beam was changed by rotating the sample around the beam axis while keeping the incident angle (6°) of the synchrotron light fixed. The XPS measurement has been carried out in normal emission geometry and grazing incidence (4°) at a photon energy of 515 eV and 1030 eV using linearly p-polarized light with a total energy resolution of 300 meV.

The clean Cu(100) surface was prepared by a standard procedure, cycles of Ar+ ion sputtering at 2.0 keV followed by annealing at 800 K. The oxygen-covered Cu(100) surface, which shows a $\sqrt{2} \times 2\sqrt{2}R45°$ reconstruction confirmed either by reflective high-energy electron diffraction (RHEED) low energy electron diffraction (LEED) pattern was prepared by exposing the Cu(100) surface to 800 L of O_2 at the sample temperature of 500 K[4].
CoTPP molecules (Porphyrin system, ≥95% purity) were thermally sublimated at 520 K from a home-made Knudsen cell type evaporator onto the copper substrate kept at room temperature. The coverage has been calibrated with a quartz micro-balance, the resulting deposition rate was 15 min/ML. The nominal coverage for all the experiments presented here is monolayer coverage. At this coverage, the ordering of the molecular layer was monitored using RHEED.
The NO_2 exposure on the molecular arrays supported by bare and oxygen modified copper surfaces was performed in the preparation chamber in the $5 \cdot 10^{-7}$ - $5 \cdot 10^{-6}$ mbar range while keeping the sample at room temperature.

The geometry optimization of title molecules has been carried out by using the Amsterdam Density Functional (ADF) software package[5] within the assumption of an idealized D_{4h} symmetry for CoTPP, C_{4v} for Cu-CoTPP, C_{2v} for CoTPP-H_2O and Cu- CoTPP-NO_2. The optimizations have been carried out by running spin-unrestricted, nonrelativistic DFT calculations with generalized gradient corrections self-consistently included through the Becke−Perdew formula[6,7] and by adopting a triple-ζ with a polarization function Slater-type basis set for all the atoms. Cu-CoTPP-NO_2 $L_{2,3}$-edges XA spectra have been modelled by evaluating *EE*s and corresponding oscillator strength distributions for transitions having the Co 2p-based MOs as initial spin orbitals with the ORCA program[8]. The DFT/ROCIS method[9] was used, which includes SOC in a molecular Russell−Saunders fashion[10], by adopting the B3LYP exchange-correlation (XC) functional[11] and by using the def2-TZVP(-f) basis set and the resolution of identity approximation (def-TZVP/J basis)[12]. The combined use of DFT and configuration interaction needs a set of three semi-empirical parameters (c_1 = 0.21, c_2 = 0.49, and c_3 = 0.29), which have been calibrated by Neese[8]. Zeroth order regular approximation has been adopted to treat the scalar relativistic effects[13]. Numerical integrations for all calculations have been carried out on a dense Lebedev grid (302 points)[14]. Finally, our attention has been concentrated on the experimental and simulated L_3-edge spectra, which do not suffer of extra broadening and distortion due to the Coster-Kronig Auger decay process[15,16].

Results and Discussion

S1. Free CoTPP and weakly interacting with oxygen

In the gas phase, CoTPP is characterized by a single unpaired electron (S = 1/2), with a Co(II) ion ($3d^7$ configuration) and a low spin (LS) state. The square planar coordination of Co(II) (D_{4h} symmetry[17]) lifts the five-fold degeneracy of the Co 3d atomic orbitals (AOs) in a_{1g} (d_{z^2}), b_{1g} ($d_{x^2-y^2}$), b_{2g} (d_{xy}) and e_g ($d_{xz,yz}$). The present ADF outcomes confirm the higher stability (0.90 eV) of the LS state compared with the high spin (HS) one. LS energy levels lying in between -6.5 eV and -2.0 eV are displayed on the left side of Figure S1 together with 3D contour plots (CP) for Co 3d-based MOs. The inspection of the figure testifies that the unpaired electron is localized on the Co $3d_{z^2}$ orbital[18] (the lowest unoccupied MO (LUMO) corresponds to the Co $3d_{z^2}$-based β orbital), while the CoTPP highest occupied molecular orbital (HOMO) is the ring based TPP-based $12a_{2u}$ MO (not shown).

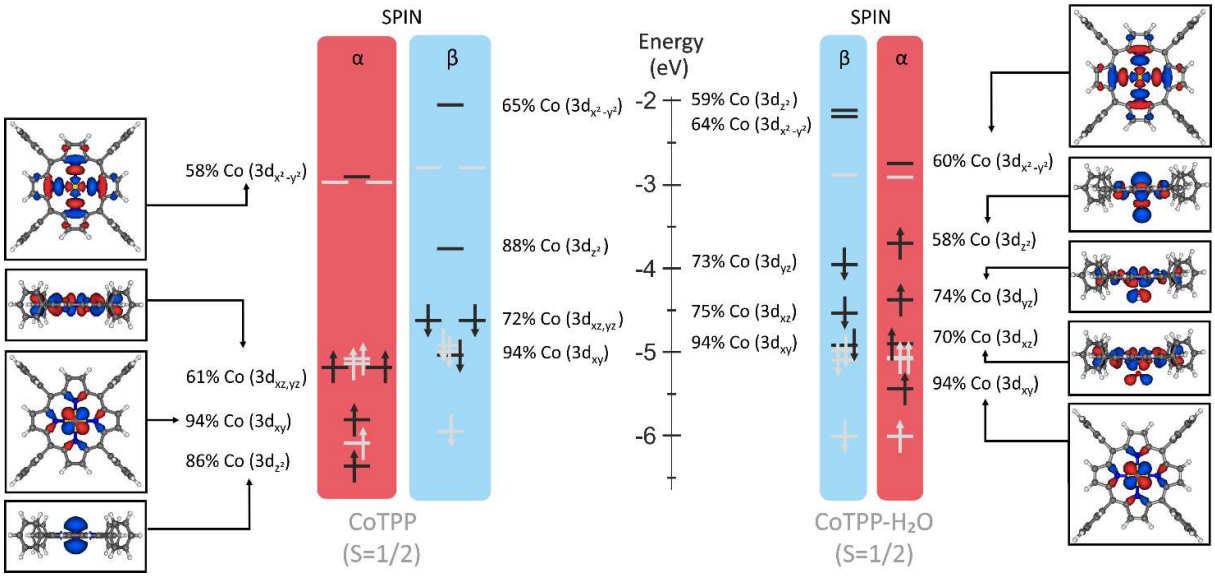

Figure S1: Energy level diagram associated to the LS CoTPP (left) and LS CoTPP-H_2O (right) species with a fixed Co-O distance at 1.6 Å (right) and optimized structures. Both α and β spins are reported. Black arrows indicate the occupied Co 3d-based α and β MOs (the relative percentage is also reported), whose 3D contour plots are displayed in the insets. The comparison between α and β spin occupation shows that the single unpaired electron is localized on the α Co $3dz^2$ MO. Grey arrows indicate the occupied α and β TPP-based MOs. No unpaired electron is localized on the TPP fragment. Colour code in Figure 1.

To get insight into the cobalt-based 3d MOs, the cluster approach has been extended to the CoTPP/O-Cu(100) system. The adoption of the molecular cluster approach to model a periodic system implies the saturation of the oxygen dangling bonds with hydrogen/pseudo-hydrogen atoms.The interaction of CoTPP with chemisorbed oxygen on the O-Cu(100) surface, which shows a (√2×2√2)R45° reconstruction, has been mimicked by considering an H_2O molecule directly bound to the Co ion. It is noteworthy that this strategy has been successfully used in the past to simulate the electronic properties of FePc at the same experimental conditions (oxygen pre-adsorbed on Cu(100))[19]. Literature data suggest that an H_2TPP monolayer grown on the oxygen passivated Cu(110) surface has an average height of 3.1 Å[20]; an internuclear distance of 1.6 Å has been chosen for Co-O bond in constrained optimization. Analogously to free CoTPP, the CoTPP-H_2O metal ion is a LS Co(II) with a single unpaired electron in the Co $3d_{z^2}$-based MO. Interestingly, the oxidation and spin states of the Co ion do not change by varying the Co-O internuclear distances from 1.3 Å to 2.0 Å. Incidentally, the Co-N^{Py} bond lengths undergo a slight lengthening in CoTPP-H_2O (2.002 Å), as compared to free CoTPP (1.978 Å). Moreover, in the CoTPP-H_2O complex, the Co(II) ion is displaced out from the N^{Py} coordinative plane by 0.19 Å. The energy level diagram for CoTPP-H_2O is displayed on the right side of Figure S1. Even if neither the Co oxidation state nor its spin state change, the opposite is true when the single Co 3d-based MOs are considered. As expected, the most relevant perturbation, a strong destabilization, is experienced by the Co $3d_{z^2}$-based MO, which points directly toward the O atom and becomes the HOMO of the CoTPP-H_2O cluster (the energy destabilization for the spin α amounts to 2.68 eV). Moreover, the Co-contribution to this MO decreases from 86% to 58% (see corresponding 3D CP in Figure S1). As such, it is of some interest to underline that, as a consequence of their partial z character, Co $3d_{xz}$- and $3d_{yz}$-based orbitals are slightly destabilized as well, but they maintain their lone pair character (70% and 74%, respectively) (see Figure S1). Analogous considerations hold for Co $3d_{xy}$- and $3d_{x2-y2}$-based MOs.

S2. Spin state stability calculation in Cu-CoTPP

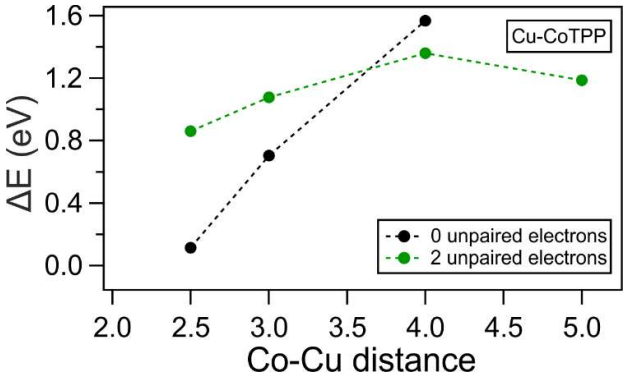

Figure S2. Energy variations of the optimized systems at different Co-Cu fixed distance and different spin state. 0 (LS) and 2 (HS) unpaired electrons are in black and green, respectively. They are expressed in eV and as a difference with respect to the most stable system: the 0 unpaired electrons with a Cu-Co distance of 2.5 Å. The 0 unpaired electrons calculation at Co-Cu=5 Å does not converge.

S3. N 1s and Co 2p core level spectra

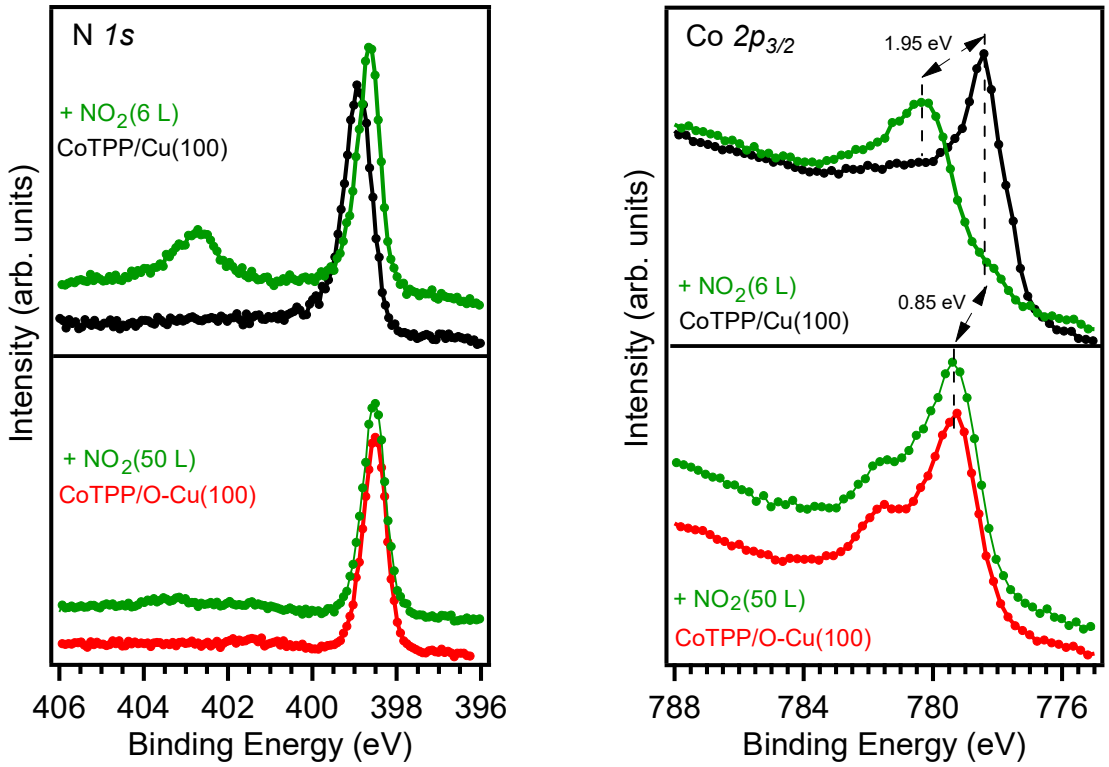

Figure S3. N 1s and Co 2p XPS core level spectra of CoTPP on bare and oxygen modified copper surfaces and after dosing of NO_2; doses are indicated.

The N 1s spectra of the pristine CoTPP on Cu(100) and oxygen modified copper surface show single sharp peaks at 398.95 and 398.50 eV, respectively, and they are assigned to the core level ionization at the four nitrogen atoms of the macrocycle metal porphyrin molecule (see Fig. S3).

When the molecular film on the bare copper surface is exposed to 6L of NO_2, a new spectral feature appears at 402.8 eV and is attributed to the nitrogen of the NO_2 molecules anchored to the Co ion of CoTPP/Cu(100) interface. This Co-NO_2 interaction is not taking place at CoTPP/O-Cu(100) interface as, after exposure to an even higher dose of NO_2 (50 L), the feature at 402.8 eV is absent in the N 1s spectra. The behavior in the N1s spectra is in agreement with the Co $2p_{3/2}$ core-level spectra discussed in the main text.

S4. NEXAFS measured Co L_3-edge for CoTPP/Cu(100) and CoTPP/O-Cu(100)

The Co L_3-edge X-ray spectra of CoTPP deposited on O-Cu(100) (see Fig. S4) shows a shape similar to that of the multilayer CoTPP reported in Ref. [21]. Analogously to free CoTPP, the CoTPP-H_2O metal ion is stabilized in LS Co^{II} configuration with a single unpaired electron in the Co $3d_{z^2}$-based MO.

Based on the present theoretical investigation, the resonances in the Co L-edge spectra measured with *p*-polarized light for the CoTPP/O-Cu(100) interface are mainly characterized by $\Delta S = 0$ electronic states and are generated by the transitions from single Co 2p to Co-based (d_{z^2}) singly occupied molecular orbitals (SOMOs). The most intense peaks in the spectrum recorded in the *s*-polarization are associated with both $\Delta S = 0$ (67%) and $\Delta S = +1$ (32%) electronic states and are assigned to Co 2p → virtual molecular orbitals (VMOs) (e_g symmetry) TPP-based single electronic transitions.

In contrast with the CoTPP on O-Cu(100) the Co L-edge NEXAFS spectrum of CoTPP deposited on bare Cu(100) manifests strikingly different behavior, both in the shape of the spectra and in the energy position of the resonances (see Fig. 4). The resonances observed in the spectra measured with p-polarized light are associated with the Co 2p → Co (d_{z^2}) electronic excitations, while the features shown in the spectra recorded with s-polarization are assigned to the transition from Co 2p to VMOs.

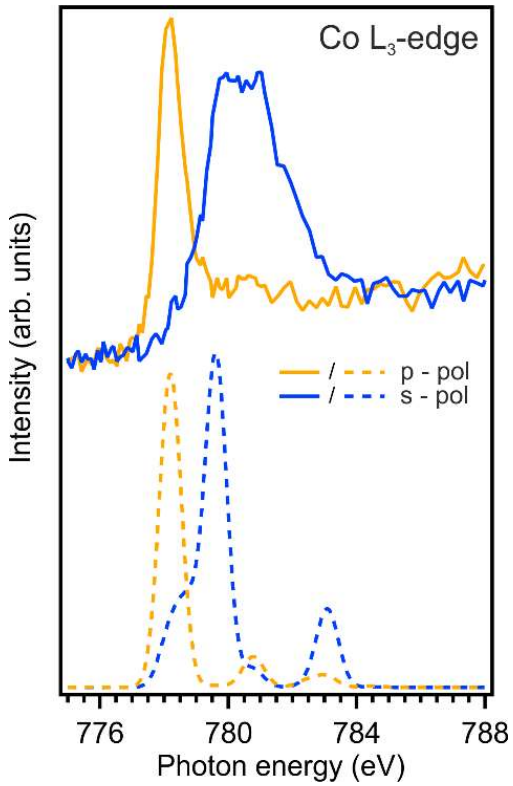

Figure S4. Measured and simulated Co *L*$_3$-edge NEXAFS spectra of CoTPP on the oxygen modified copper surface measured at p- and s- polarization of incoming light. To match the experimental data, the simulated spectra for CoTPP-H_2O (dashed line) are shifted by 2.3 eV and have a Gaussian broadening of 0.8 eV.

S5. Optimized geometries

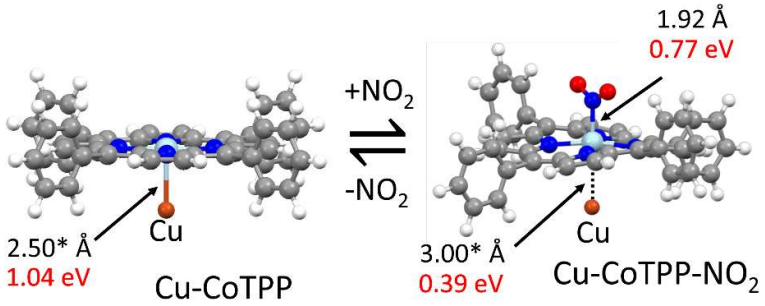

Figure S5. Optimized geometries of clusters associated with the transformations considered in the present work. Binding energies and bond lengths of Cu-CoTPP and Cu-CoTPP-NO_2 are described at BP86/TZVP level of theory. Both structures are in their LS states. Grey, white, orange, red, light blue and blue spheres are representative of C, H, Cu, O, Co and N atoms, respectively. Asterisks (*) refer to constrained optimization geometries.

S6. The isolated CoTPP-NO_2: the direct comparison with isolated NO_2 and Cu-CoTPP-NO_2

Both CoTPP and NO_2 are open-shell molecules each of them carrying a single unpaired electron: two spin states are then possible for the CoTPP–NO_2 complex: either a LS state with no unpaired electron or a HS state with two unpaired electrons. Geometry optimizations have been carried out for both spin state and by assuming a Co–NO_2 direct interaction (Y-shaped coordination)[22]. The LS state has been estimated more stable than the HS one by 0.92 eV; moreover, the Co–NO_2 binding energy (BE) amounts to 1.31 eV, while optimized Co–NO_2 and N–O bond lengths (BL) are 1.88 and 1.23 Å, respectively (the optimized N–O BL of the free NO_2 is 1.21 Å). The analysis of the CoTPP–NO_2 frontier orbitals reveals that the Co–NO_2 bond formation is accompanied by the Co(II) → Co(III) oxidation. In more detail, the CoTPP–NO_2 lowest unoccupied MO (LUMO, see the left side of Figure S6), is strongly localized on the Co $3d_{z^2}$ (46%, singly occupied in CoTPP), while the $\pi^*_{\|}$ NO_2-based MO (singly occupied in NO_2, see the left side of Figure S6) is doubly occupied[23].

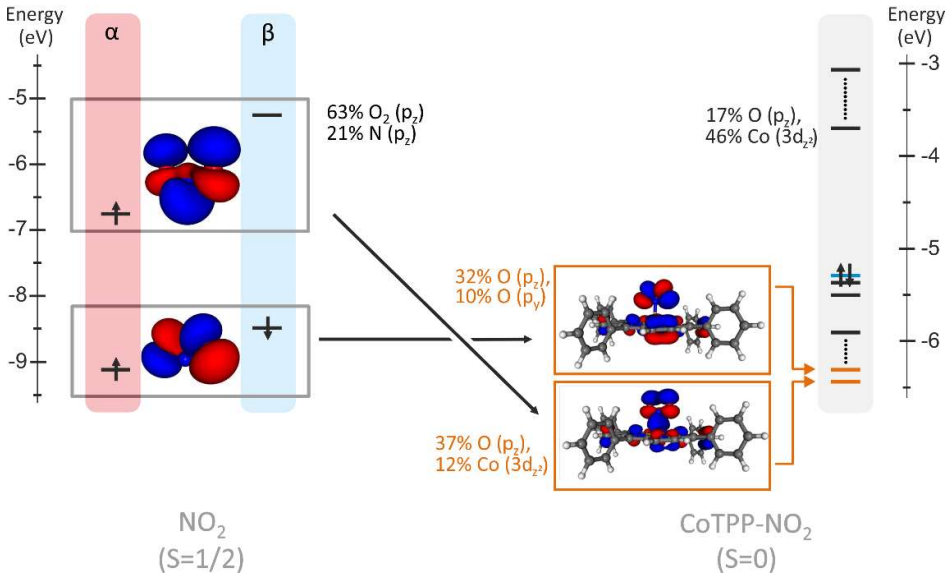

Figure S6. *Energy level diagrams of LS CoTPP-NO_2 complex (left) and NO_2 molecule (right). Both α and β spins are reported for NO_2, while CoTPP-NO_2 is a closed shell system. Black arrows indicate the electrons. In CoTPP-NO_2, all the MOs under HOMO level are doubly occupied, the double arrows are omitted for clarity. 3D contour plots are displayed only for NO_2-based MOs. The black levels are mainly localized on the Co (3d), while the orange ones on NO_2. The TPP-based levels are omitted (except for the HOMO, blue level). Vertical dots indicate that some levels, localized on TPP fragment, are omitted. Colour code in Figure 1.*

The inspection of NO_2-based MOs upon moving from the CoTPP-NO_2 complex to the Cu-CoTPP-NO_2 cluster provides further insights into the role played by the surface after the NO_2 coordination. The adsorption of CoTPP on Cu implies the redox reaction Co(II) + Cu(0) → Co(I) + Cu(I) (see main text for the detailed discussion). The bonding of NO_2 to Cu(I)-Co(I)TPP, mimicked by the Cu-CoTPP-NO_2 cluster, changes again the Co and Cu (Co(I) → Co(III)) and Cu (Cu(I) → Cu(0)) oxidation states. The Co(III) species present in the Cu-CoTPP-NO_2 cluster is six-fold coordinated, even if the Cu–Co bonding is rather weak. Such a picture is perfectly consistent with BE

and ^{NM}I variations (see main text) as well as with the MO evolution upon moving from CoTPP-NO_2 to Cu-CoTPP-NO_2 (see Figure S7). In more detail, the inspection of Figure S7 clearly testifies that: i) NO_2-based MOs (orange levels) have very similar energies and compositions, thus indicating the net transfer of an electron to the $\pi^*_{||}$ NO_2-based MO in both cases; ii) the Cu 4*s*-based MO (green levels) is singly occupied, thus ultimately testifying the Cu(0) oxidation state; iii) the Co 3*d*-based MOs (black levels) in CoTPP-NO_2 and Cu-CoTPP-NO_2 have quite similar energies and composition, thus confirming that Co has the same oxidation state (+3) in CoTPP-NO_2 and Cu-CoTPP-NO_2. Minor differences can be traced back to the weak interaction with Cu.

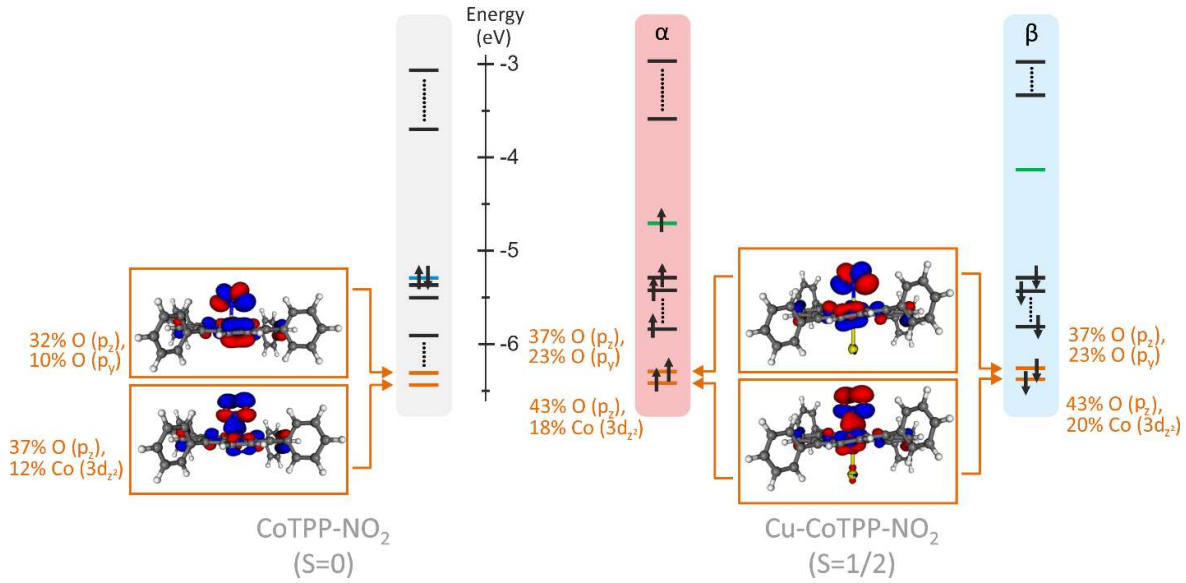

Figure S7. *Energy level diagrams associated to the isolated LS CoTPP-NO_2 (left) and Cu-CoTPP-NO_2 (right) species. Both α and β spins are reported for Cu-CoTPP-NO_2, while the CoTPP-NO_2 species has not unpaired electron. Black arrows indicate the electrons. In CoTPP-NO_2, all the MOs under HOMO level are doubly occupied, the double arrows are omitted for clarity. 3D contour plots are displayed only for NO_2-based MOs. The black levels are mainly localized on the Co (3d), the green ones on Cu (4s), while the orange ones on NO_2. The TPP-based levels are omitted (except for the CoTPP-NO_2 HOMO, blue level). Vertical dots indicate that some levels, localized on TPP fragment, are omitted. Colour code in Figure 1.*

S8. The Nalewajski-Mrozek bond multiplicity index (^{NM}I)

	$^{NM}I_{Co\text{-}N(TPP)}$	$^{NM}I_{Co\text{-}Cu}$	$^{NM}I_{Co\text{-}NO2}$
Cu-CoTPP	0.61	0.95	//
CoTPP-NO_2	0.59	//	0.69
Cu-CoTPP-NO_2	0.58	0.16	0.61

Table S8. *The Nalewajski-Mrozek bond multiplicity indexes (^{NM}I) for Cu-CoTPP, CoTPP-NO_2 and Cu-CoTPP-NO_2 systems.*

S9. Comparison between measured and calculated momentum maps for CoTPP/Cu(100)

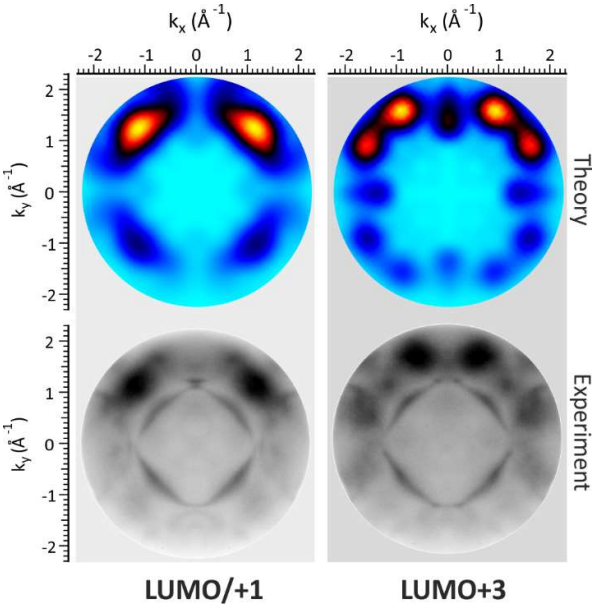

Figure S9. Comparison between the measured momentum resolved photoemission maps at constant BE (0.15 eV and 0.80 eV, respectively) and the square modulus of the Fourier transform of the real space molecular orbitals (LUMO/+1 and LUMO+3) provided by DFT calculation, within the photoemission tomography (PT) approach. MO can be found at http://143.50.77.12:5000.

S10. Co 2p $_{3/2}$ and N1s core level spectra, annealing experiment

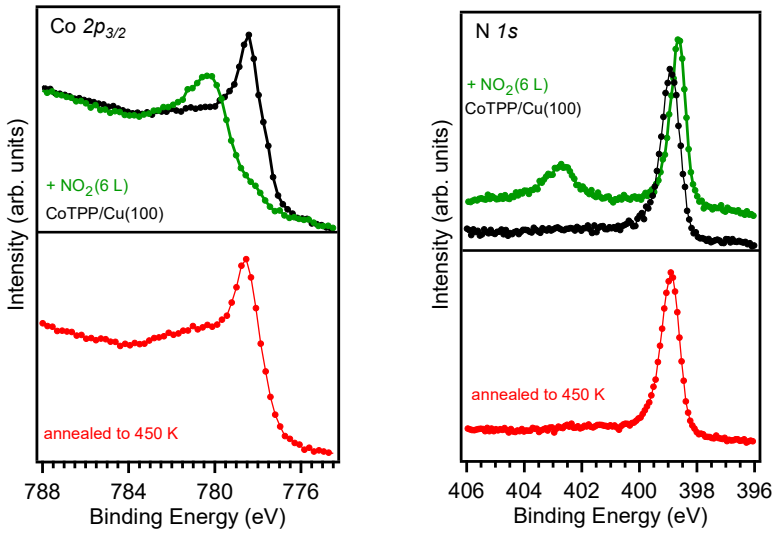

Figure S10. Top: Co $2p_{3/2}$ and N 1s XPS core-level spectra of CoTPP on Cu(100) and after dosing of NO_2; Bottom: after annealing of NO_2-CoTPP/Cu(100) interface to 450 K for thermal desorption of NO_2 ligand.

References

[1] C. M. Schneider, C. Wiemann, M. Patt, V. Feyer, L. Plucinski, I. P. Krug, M. Escher, N. Weber, M. Merkel, O. Renault, N. Barrett, *J. Electron Spectros. Relat. Phenomena* **2012**, *185*, 330–339.

[2] L. Floreano, G. Naletto, D. Cvetko, R. Gotter, M. Malvezzi, L. Marassi, A. Morgante, A. Santaniello, A. Verdini, F. Tommasini, G. Tondello, *Rev. Sci. Instrum.* **1999**, *70*, 3855–3864.

[3] L. Floreano, A. Cossaro, R. Gotter, A. Verdini, G. Bavdek, F. Evangelista, A. Ruocco, A. Morgante, D. Cvetko, *J. Phys. Chem. C* **2008**, *112*, 10794–10802.

[4] M. Wuttig, R. Franchy, H. Ibach, *Surf. Sci.* **1989**, *213*, 103–136.

[5] H. S. Rzepa, *Annu. Reports Prog. Chem. - Sect. B* **1980**, *77*, 15–26.

[6] A. D. Becke, *Phys. Rev. A* **1988**, *38*, 3098–3100.

[7] J. P. Perdew, *Phys. Rev. B* **1986**, *33*, 8822–8824.

[8] M. Yamada, M. Foote, T. W. Prow, *Wiley Interdiscip. Rev. Nanomedicine Nanobiotechnology* **2015**, *7*, 428–445.

[9] M. Roemelt, F. Neese, *J. Phys. Chem. A* **2013**, *117*, 3069–3083.

[10] M. Roemelt, D. Maganas, S. Debeer, F. Neese, *J. Chem. Phys.* **2013**, *138*, 204101.

[11] A. D. Becke, *J. Chem. Phys.* **1993**, *98*, 5648–5652.

[12] F. Weigend, R. Ahlrichs, *Phys. Chem. Chem. Phys.* **2005**, *7*, 3297–3305.

[13] D. A. Pantazis, X. Y. Chen, C. R. Landis, F. Neese, *J. Chem. Theory Comput.* **2008**, *4*, 908–919.

[14] V. I. Lebedev, *USSR Comput. Math. Math. Phys.* **1975**, *15*, 44–51.

[15] D. Coster, R. De L. Kronig, *Physica* **1935**, *2*, 13–24.

[16] D. Maganas, M. Roemelt, T. Weyhermüller, R. Blume, M. Hävecker, A. Knop-Gericke, S. Debeer, R. Schlögl, F. Neese, *Phys. Chem. Chem. Phys.* **2014**, *16*, 264–276.

[17] Y. H. Chang, H. Kim, S. J. Kahng, Y. H. Kim, *Dalt. Trans.* **2016**, *45*, 16673–16681.

[18] T. Lukasczyk, K. Flechtner, L. R. Merte, N. Jux, F. Maier, J. M. Gottfried, H. P. Steinrück, *J. Phys. Chem. C* **2007**, *111*, 3090–3098.

[19] I. Cojocariu, S. Carlotto, H. M. Sturmeit, G. Zamborlini, M. Cinchetti, A. Cossaro, A. Verdini, L. Floreano, M. Jugovac, P. Puschnig, C. Piamonteze, M. Casarin, V. Feyer, C. M. Schneider, *Chem. - A Eur. J.* **2021**, *27*, 3526–3535.

[20] M. Wagner, P. Puschnig, S. Berkebile, F. P. Netzer, M. G. Ramsey, *Phys. Chem. Chem. Phys.* **2013**, *15*, 4691–4698.

[21] G. Fratesi, S. Achilli, A. Ugolotti, A. Lodesani, A. Picone, A. Brambilla, L. Floreano, A. Calloni, G. Bussetti, *Appl. Surf. Sci.* **2020**, *530*, 147085.

[22] M. H. Chang, N. Y. Kim, Y. H. Chang, Y. Lee, U. S. Jeon, H. Kim, Y. H. Kim, S. J. Kahng, *Nanoscale* **2019**, *11*, 8510–8517.

[23] I. M. Sharafeldin, N. K. Allam, *New J. Chem.* **2017**, *41*, 14936–14944.